

Brittle-Ductile Transition in Intrinsic Fracture Behavior of Crystals

Kin S. Cheung and Sidney Yip

Department of Nuclear Engineering, Massachusetts Institute of Technology, Cambridge, Massachusetts 02139

(Received 3 August 1990)

A transition of brittle to ductile propagation of a sharp crack in a crystal is observed by molecular-dynamics simulation and the transition mechanism shown to be the emission of dislocations at the crack tip and activation of specific slip systems appropriate to the crystal structure. Implications for extension of current theories are discussed.

PACS numbers: 62.20.Mk, 46.30.Nz, 62.20.Fe, 81.40.Np

A crystal is said to be intrinsically brittle if an existing crack is able to propagate along a crystallographic plane in a cleavage manner when the solid is under stress. On the other hand, the crystal is considered to be ductile if the crack-tip extension is accompanied by plastic deformation. While transitions from brittle to ductile behavior have been observed in a number of materials,¹⁻³ this basic phenomenon, despite its obvious technological interest, is not well understood in the mechanistic aspects of dislocation nucleation and mobility.³⁻⁵ It is recognized that existing models of dislocation nucleation, based on continuum mechanics, are lacking in the atomistic treatment of thermal and nonlinear stress effects in the vicinity of the crack tip; on the other hand, such local information is not available experimentally or theoretically.

In this Letter we report a molecular-dynamics study of the response of a crystal containing a sharp crack to varying stress and temperature. A transition from brittle to ductile fracture occurring over a limited temperature range is directly observed. Detailed analyses of the atomic displacements generated by the simulation reveal the transition mechanism to be the emission of dislocations from the crack tip, the characteristics of which depend on the crystal structure and the crack orientation. As the transition implies an activation barrier for dislocation nucleation, we find that the existing continuum description⁴ is unable to account for the magnitude of the activation energy. We also show that thermal fluctuation and local stress effects play an important role in significantly reducing the overestimate of the activation energy.⁶

The general setup of our crack-tip simulation is illustrated schematically in Fig. 1. We imagine a sharp crack embedded in a crystalline material of macroscopic dimensions which is subjected to uniaxial tension. The simulation cell covers only the crack-tip region; it contains N atoms which interact with each other through a prescribed interatomic potential function. The coupling between these atoms and the surrounding medium external to the cell is expressed through a set of external forces imposed on atoms at the borders of the cell. These forces, determined at the outset and held constant

during the simulation, represent the interactions between the atoms in the simulation cell and those in the surrounding medium when all the atoms are displaced according to the linear-elasticity solutions to the crack-tip problem.⁷ The advantage of this particular border condition⁸ is that the simulation cell, with the surrounding medium removed during the simulation, is free to deform in response to the stresses generated at the crack tip as the crack propagates. In the present study the previous implementation of this border treatment⁸ has been improved to ensure the stability of the corners of the simulation cell.⁶

The interatomic potential adopted for this work has been constructed using a version of the effective-medium approximation for the bcc metal α -iron.⁹ The potential was fitted to give the experimental values of lattice parameter and sublimation energy precisely, and elastic constants and vacancy formation energy reasonably well. In our data analysis and interpretation we do not use experimental values for any of the physical parameters; for self-consistency all numerical values of physical properties are obtained directly from the model potential function.

We have examined three crack-tip configurations in the bcc crystal lattice; these will be labeled as [100](001), [110](001), and [100](011) cracks, where the crack front direction is specified and the plane is that in which the crack lies (see Fig. 5 below for an illustra-

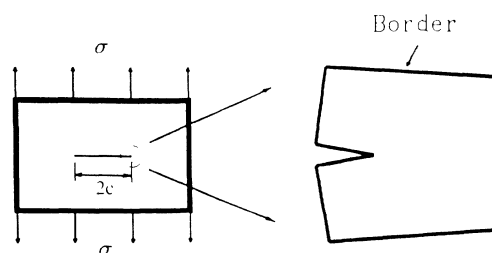


FIG. 1. Schematic of a macroscopic body containing an atomically sharp crack of length $2c$ subject to tensile stress σ (left-hand figure) and the molecular-dynamics simulation cell representing the crack-tip region (right-hand figure).

tion).⁶ The simulation cell is taken to be periodic in the direction along the crack front. Because we are simulating the condition of plane strain, most of the configurations are 2 to 4 atom layers in this direction.

A typical simulation run consists of setting up the crack-tip configuration according to the elasticity solution for the atomic displacements⁷ at a prescribed level of applied tensile stress, expressed as the quantity $K_I = \sigma\sqrt{\pi c}$, the stress intensity factor for mode I fracture. The atoms are then allowed to move according to Newton's equations of motion with the system temperature maintained at a constant value by rescaling the particle velocities after every time step of the simulation. If K_I is greater than the threshold value for the crack to

propagate, interatomic bonds will begin to break at the crack tip.¹⁰ On the other hand, if the stress is below the threshold level, one will see crack healing through the formation of new bonds.

In the case of brittle fracture a well-known criterion for the critical stress required for crack extension has been derived from an equilibrium condition between strain-energy release rate and twice the surface free energy of the crack surface.¹¹ For an isotropic medium the predicted critical value of K , K_{Ic} , depends only on the Young's modulus, the surface energy γ , and the Poisson ratio. When the anisotropic effects of a discrete crystal lattice are taken into account,⁷ the Griffith criterion becomes

$$K_{IG} = \sqrt{2\gamma} \{ (s_{11}s_{22}/2)^{1/2} [(s_{22}/s_{11})^{1/2} + (2s_{12} + s_{66})/2s_{11}]^{1/2} \}^{-1/2}, \tag{1}$$

where s_{ij} are the compliance constants with indices 1, 2, and 6 referring to the directions of plane strain, crack propagation (normal to crack front), and normal of the crack plane, respectively. In Fig. 2 we show for all three crack orientations the number of bonds broken or formed at various stress intensity values observed during a fixed interval of simulation. Broken bonds indicate that the crack is propagating under the imposed stress, while healed bonds indicate that the crack is receding. At the critical stress the crack should be stationary. It is seen that Eq. (1) is satisfied to within about 5%, which is a significant improvement over previous studies which showed deviations ranging from 20% to a factor of 3.⁸ We regard this agreement as an indication of physical meaningfulness of our simulation model, particularly concerning the treatment of the border condition and the

anisotropy of the crack-tip structure.

To study the transition from brittle to ductile fracture we examine each crack tip at a supercritical stress value of $1.1K_{IG}$ over a range of temperatures. In these runs the number of atoms in the cell ranges from 2400 to 3000, with corresponding cell dimensions ranging from $120 \text{ \AA} \times 80 \text{ \AA}$ to $120 \text{ \AA} \times 120 \text{ \AA}$ in the two directions shown in Fig. 3. At low temperatures brittle cleavage is observed in all cases. An example of cleavage fracture is given in Fig. 3, which shows the instantaneous atomic positions of a $[100](0\bar{1}1)$ crack after 3000 time steps (4.4 psec) of simulation at $T=200 \text{ K}$. The atomic configuration of the same crack simulated at $T=400 \text{ K}$

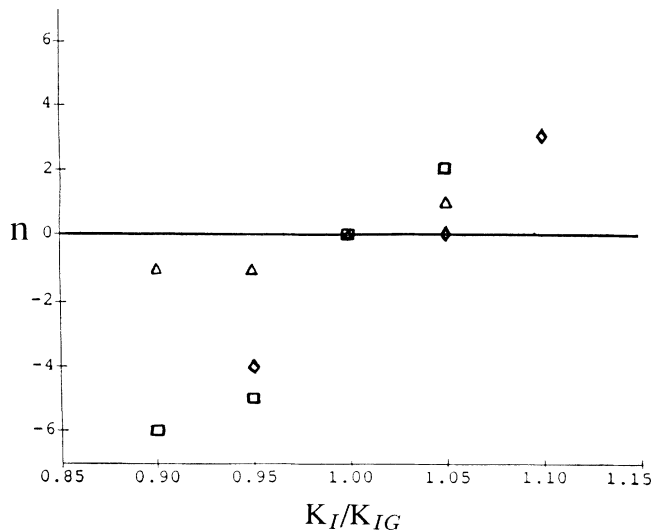


FIG. 2. Number of bonds broken (n positive) or formed (n negative) during 4.4 psec of simulation at various stress intensity factors K_I/K_{IG} ; diamonds, squares, and triangles refer to $[100](0\bar{1}1)$, $[110](001)$, and $[100](001)$ cracks, respectively.

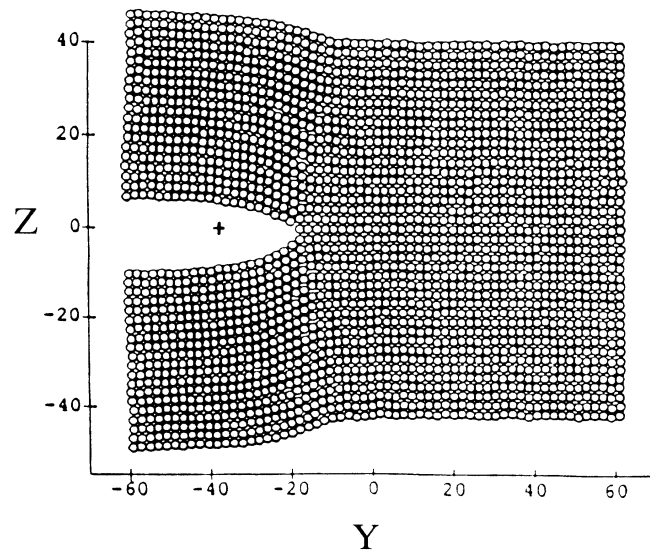


FIG. 3. Brittle fracture of a $[100](0\bar{1}1)$ crack at $T=200 \text{ K}$ and $K_I/K_{IG}=1.1$; instantaneous atomic configuration at time step 3000. The ordinate and abscissa are Z and Y axes (see Fig. 5) with scales in units of angstroms. The cross indicates the initial position of the crack tip.

is shown in Fig. 4. Here one sees clearly the presence of two edge dislocations and a significant opening of the crack tip; both are characteristic features of ductile fracture.

The transition from brittle to ductile behavior as the temperature is increased is also observed in the other two crack-tip orientations.⁶ While the transition temperature is found to be somewhat different in each case, the fact that the transition occurs around room temperature is in agreement with available data.² To determine the deformation mechanism associated with the transition, a detailed analysis of the atomic trajectories during the transition is carried out. We choose to work with the $[100](0\bar{1}1)$ crack because in this case the analysis is considerably simplified by the fact that the slip planes are inclined at 90° .

From the simulation data on the $[100](0\bar{1}1)$ crack model, dislocations are observed to be emitted from the crack tip with line direction parallel to the crack front direction of $[100]$. From the time trajectories of the atoms in adjacent (011) slip planes, one can discern appreciable movements in both the $[100]$ and $[0\bar{1}1]$ directions, thus suggesting the presence of a screw component of the dislocation in addition to the edge component. We have developed a method for the quantitative characterization of dislocations through the use of an atomic registry function which is a measure of the relative displacement between corresponding atomic sites across the slip plane.⁶ With this method we find the dislocations nucleated from the $[100](0\bar{1}1)$ crack to have mixed edge and screw components with Burgers vector \mathbf{b} in the

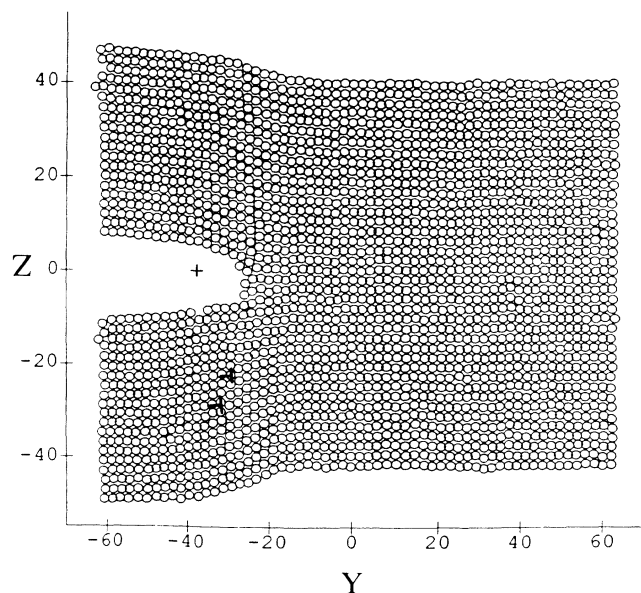


FIG. 4. Ductile fracture of a $[100](0\bar{1}1)$ crack (same as Fig. 3) at $T=400$ K and $K_I/K_{IC}=1.1$; instantaneous atomic configuration at time step 3000. Two dislocations nucleated from the crack tip are marked.

$\frac{1}{2}[1\bar{1}1]$ direction, as shown in Fig. 5. The analysis therefore confirms that in the simulation dislocations are indeed nucleated from the crack tip and they move away by gliding on the (011) plane; the $\langle 111 \rangle\{011\}$ slip in this process is known from crystallography as well as experimental observations¹² to be a major slip system for bcc crystals. It is interesting to note that although our particular choice of crack plane is not the conventional (001) cleavage plane for bcc iron, nevertheless, the deformation mechanism activated in our simulation of ductile fracture involves the same slip systems as observed in experiments.

Current understanding of the brittle-to-ductile transition is based on the model of Rice and Thomson,^{4,5} which describes the change in the free energy ΔG of the crack system resulting from the creation of a dislocation half-loop, $\Delta G(z) = U_\perp(z) + U_l(z) - U_\sigma(z)$, where $U_\perp(z)$ is the elastic self-energy of the dislocation loop of size z , U_l is the energy required to form a ledge as the loop expands to the surface, and U_σ is the energy gained by the loop in the stress field of the crack tip. If one considers a crack in an isotropic material and the formation of a half-square dislocation loop on a glide plane perpendicular to the crack plane,⁴ the expression for the elastic line energy of a planar, square dislocation loop of length L is $U_\perp \approx aL \ln(cL)$, where a is a function of the elastic constants and c is a factor which contains the cutoff distance for the dislocation core.¹³ For U_l one can simply take $\gamma b_e L$, γ being the free surface energy and b_e the edge component of the Burgers vector. For U_σ an expression based on elasticity is $a_\sigma L \sqrt{L}$, where a_σ is another func-

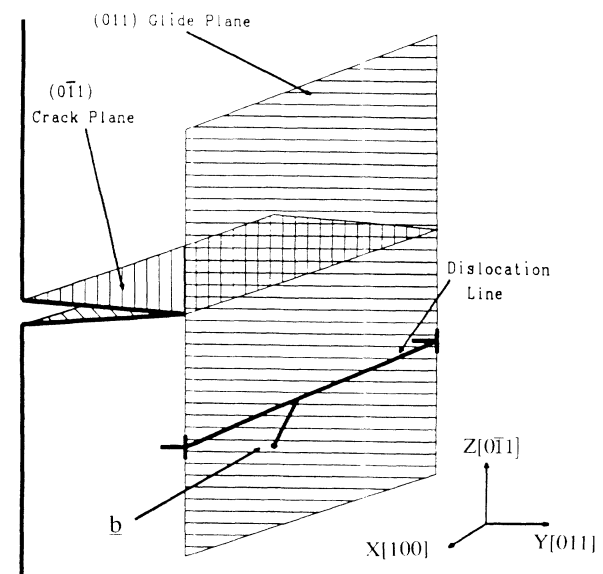


FIG. 5. Schematic showing dislocations with Burgers vector $\mathbf{b} = \frac{1}{2}[1\bar{1}1]$ gliding on the (011) plane, the mechanism of ductile fracture deduced from the simulation data on the propagation of a $[100](0\bar{1}1)$ crack.

tion of the elastic constants.⁴ The term U_σ will eventually dominate at sufficiently large loop, so $\Delta G(z)$ rises from zero at z_0 , the core cutoff, reaches a peak at a value z^* , and decreases to negative values at large z . The loop size z^* characterizes the activated or saddle-point configuration with corresponding activation energy barrier $\Delta G^* \equiv \Delta G(z^*)$. Combining the three estimates above with typical numerical values for α -iron we obtain a value of 80 eV for ΔG^* .⁶ This translates into a transition temperature of several hundred thousand degrees, clearly incompatible with observation.

We have introduced several modifications of the Rice-Thomson model using softened elastic constants at finite temperatures and stress, and the nonlinear stress distribution at the crack tip, both obtained by simulation.^{6,14} Thus in U_\perp the coefficient a becomes a function of temperature and the local stress distribution, and U_σ becomes $a_\sigma(T) \int dr \sigma_{r\varphi}(r)$, where $a_\sigma(T)$ accounts for the thermal softening of the elastic constants and $\sigma_{r\varphi}(r)$ is the stress distribution calculated directly by molecular dynamics. These modifications give a significantly reduced value of ΔG^* , approximately 5 eV. Although such a barrier height is still too large to account for the observed transition, our analysis clearly points to the important role of thermal and stress softening effects and that of nonlinear stress distribution.

In summary, we have demonstrated that while continuum mechanics and elasticity provide an appropriate framework for the description of intrinsic fracture behavior of crystalline solids, an integrated approach incorporating the atomic-level information available from molecular dynamics is necessary to achieve a level of quantitative understanding.

We would like to acknowledge long-standing collaboration with A. S. Argon, and very helpful discussions with J. R. Rice. K.S.C. acknowledges the support of an NSF Graduate Fellowship; this work was also supported in part by the National Science Foundation through

Grants No. CHE-8806767 and No. CES-8815942. Computer usage was mainly provided by allocations from the San Diego Supercomputer Center, with some early support from DOE Grant No. DE-FG02-87ER45294-A003.

¹G. T. Hahn, B. L. Averbach, W. S. Owen, and M. Cohen, in *Fracture*, edited by B. L. Averbach *et al.* (Technology Press, MIT, Cambridge, MA, 1959), p. 91.

²*Mechanical Behavior of Materials*, edited by F. A. McClintock and A. S. Argon (Addison-Wesley, Reading, 1966), p. 561.

³P. B. Hirsch, S. G. Roberts, and J. Samuels, *Proc. Roy. Soc. London A* **421**, 25 (1989).

⁴J. R. Rice and R. Thomson, *Philos. Mag.* **29**, 73 (1974).

⁵A. S. Argon, *Acta Metall.* **35**, 185 (1987).

⁶K. S. Cheung, Ph.D. thesis, MIT, 1990 (unpublished).

⁷G. C. Sih and H. Liebowitz, in *Fracture: An Advanced Treatise*, edited by H. Liebowitz (Academic, New York, 1968), Vol. 2, p. 67.

⁸B. deCelis, A. S. Argon, and S. Yip, *J. Appl. Phys.* **54**, 4864 (1983).

⁹R. J. Harrison, A. F. Voter, and S. P. Chen, in *Atomistic Simulation of Materials—Beyond Pair Potentials*, edited by V. Vitek and D. J. Srolovitz (Plenum, New York, 1989), p. 219; this approach of constructing potential functions is also known as the embedded-atom method; see M. S. Daw and M. I. Baskes, *Phys. Rev. B* **29**, 6443 (1984).

¹⁰An interatomic bond across the crack plane is considered broken if the atom separation exceeds 1.5 times the distance in the equilibrium stress-free crystal; similarly, a bond is considered formed when the separation between a pair of atoms becomes less than this amount.

¹¹A. A. Griffith, *Philos. Trans. Roy. Soc. A* **221**, 163 (1920).

¹²S. M. Ohr, *Mater. Sci. Eng.* **72**, 1 (1985).

¹³J. P. Hirth and J. Lothe, *Theory of Dislocations* (Wiley, New York, 1968).

¹⁴K. S. Cheung, A. S. Argon, and S. Yip, *J. Appl. Phys.* (to be published).